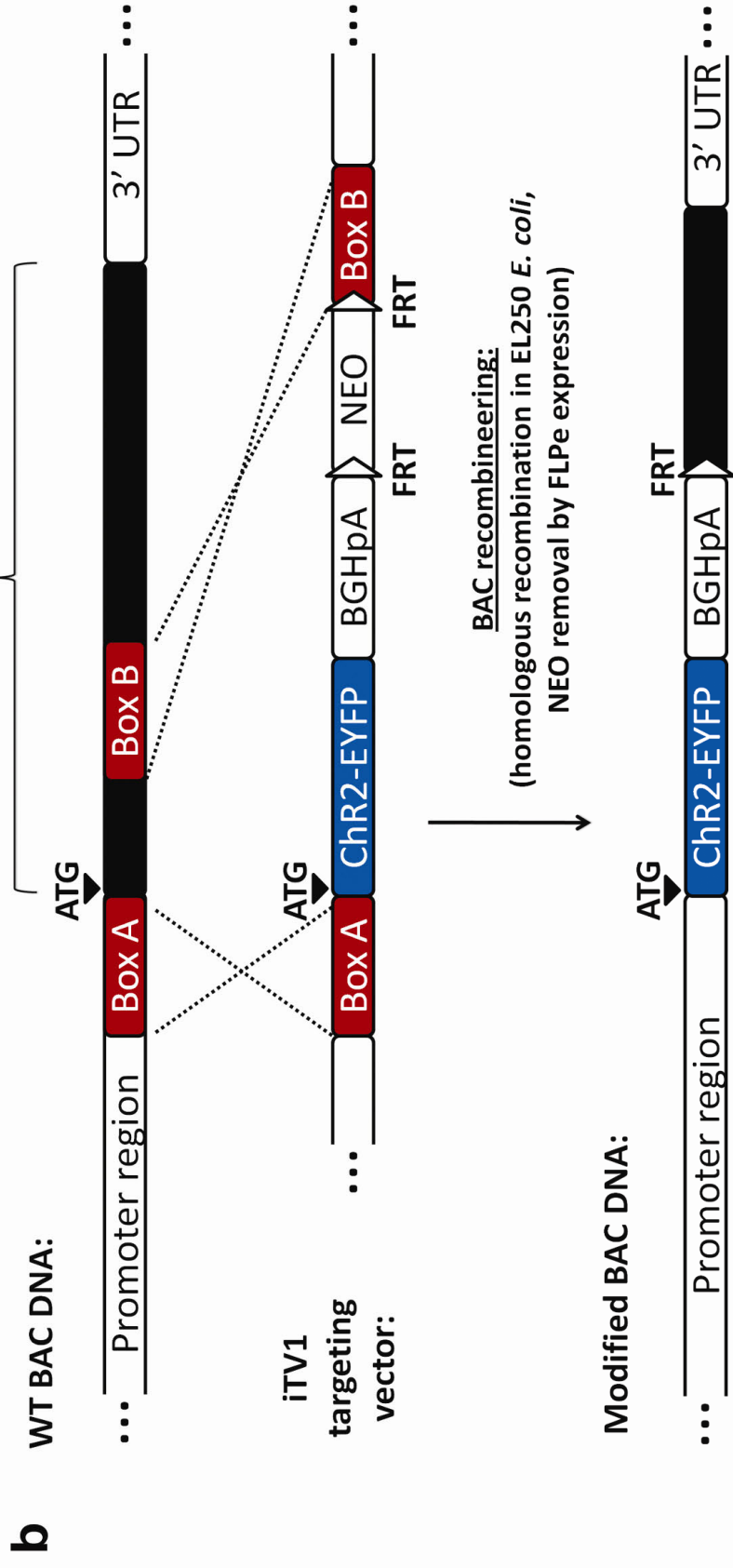
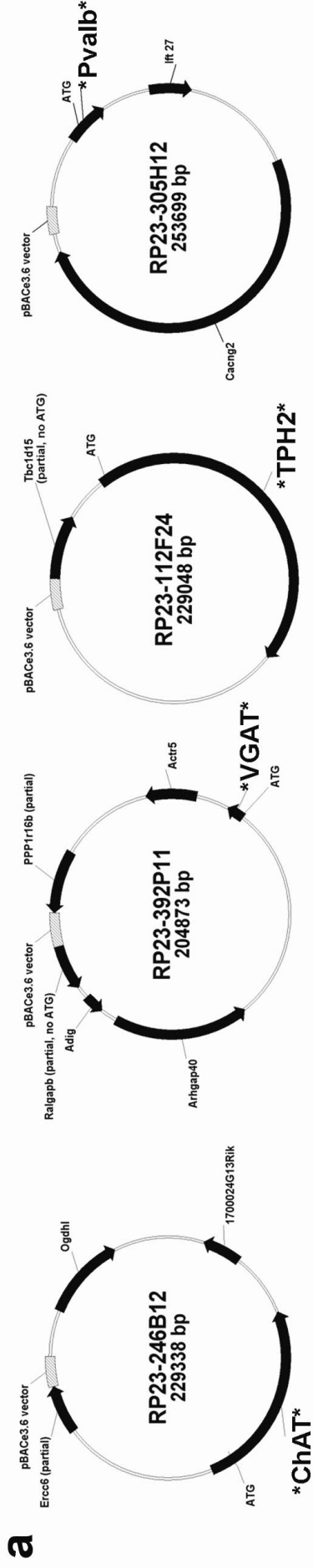


# Zhao et al., Supplementary Figure 1

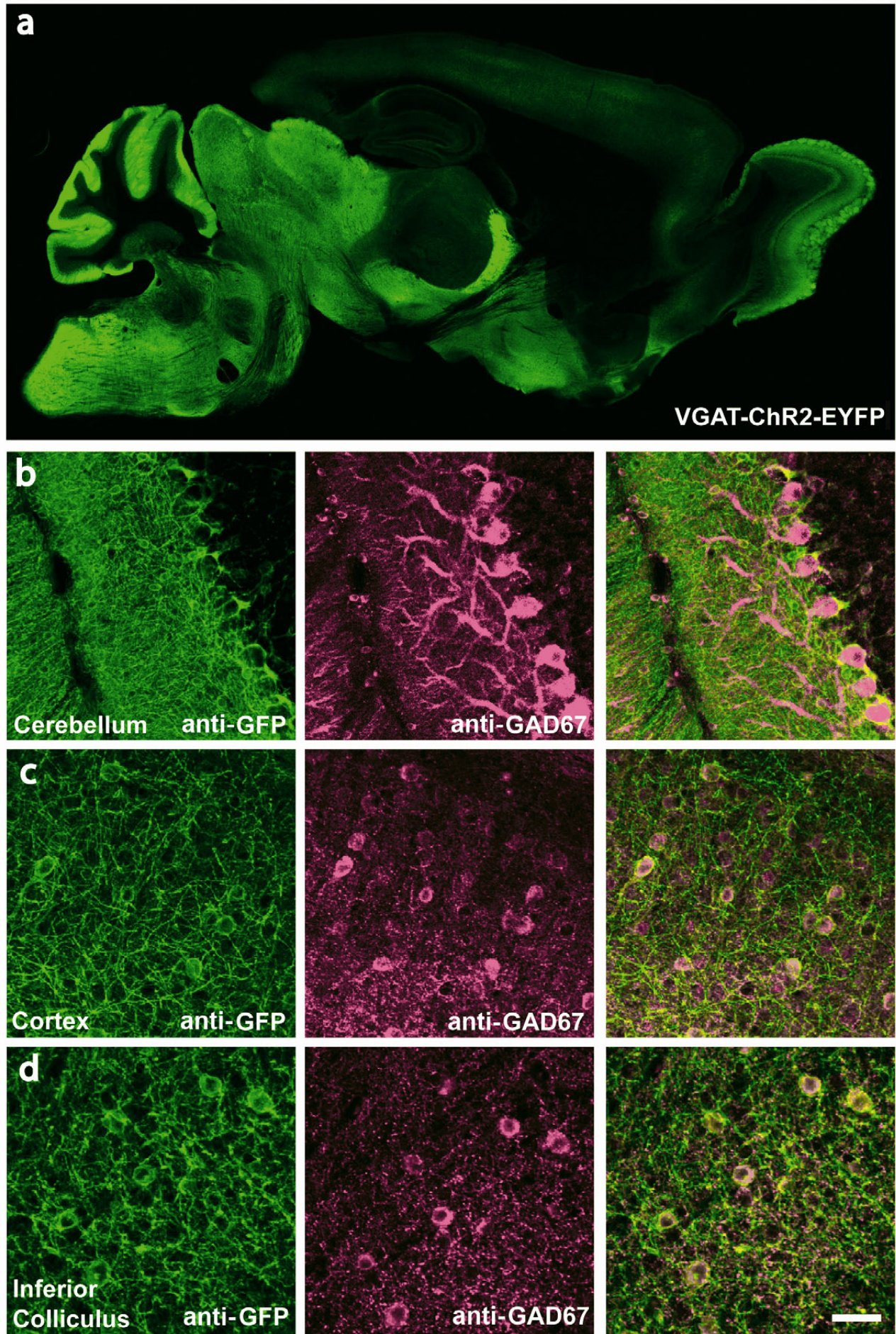


**Supplementary Figure 1.** Overview of BAC clones and targeting strategy for generation of cell-type specific ChR2(H134R)-EYFP BAC transgenic mice. **(a)** Diagram of BAC clones used in this study. All BAC clones are from the RP23 library and contain the pBACe3.6 vector backbone. **(b)** Overview of the general BAC modification strategy to introduce ChR2(H134R)-EYFP under the control of the cell-type specific promoter elements. The vector iTV1 was used to introduce the ChR2(H134R)-EYFP-BGHpA-FRT-NEO-FRT cassette immediately upstream of the known translation initiation site (labeled ATG) for each targeted gene in the four different BAC clones. Each targeting vector contains BAC-specific Box A and Box B fragments for homologous recombination in the EL250 strain of *E. coli*. The presence of the FRT-NEO-FRT confers kanamycin resistance for selection of EL250 cells containing the properly targeted BACs. The NEO cassette is subsequently removed by arabinose-induced FLPe expression in the EL250 cells, thereby leaving only a single residual FRT site.

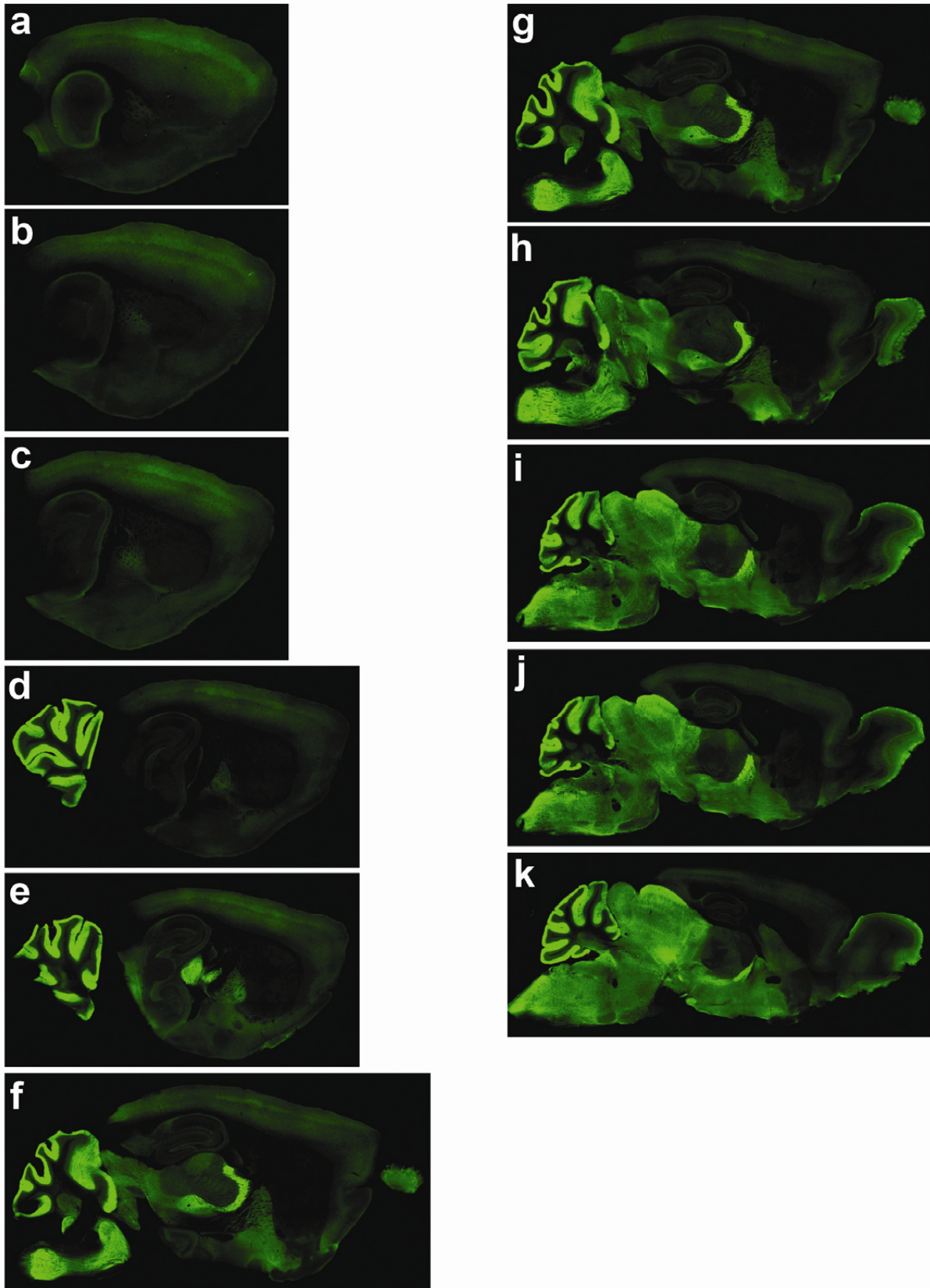
**Supplementary Figure 2.** Characterization of ChR2-EYFP expression in *VGAT-ChR2(H134R)-EYFP* line 8 BAC transgenic mice. **(a)** Mouse brain sagittal image to show strong ChR2-EYFP expression in the glomerular and mitral cell layers of the olfactory bulb, thalamic reticular nucleus (TRN), superior and inferior colliculus, the molecular layer of the cerebellum and brainstem, and moderate expression in the cortex, hippocampus, thalamus and the granule cell layer of the olfactory bulb. **(b-d)** Confocal images showing the precise colocalization of ChR2-EYFP and GAD67 in the molecular layer of the cerebellum **(b)**, cortex **(c)** and superior colliculus **(d)**. Left panel: anti-GFP staining; middle panel: anti-GAD67 staining; right panel: merged image of anti-GFP and anti-GAD67 staining. Scale bar: 100  $\mu$ m.

**(See next page →)**

Zhao et al., Supplementary Figure 2

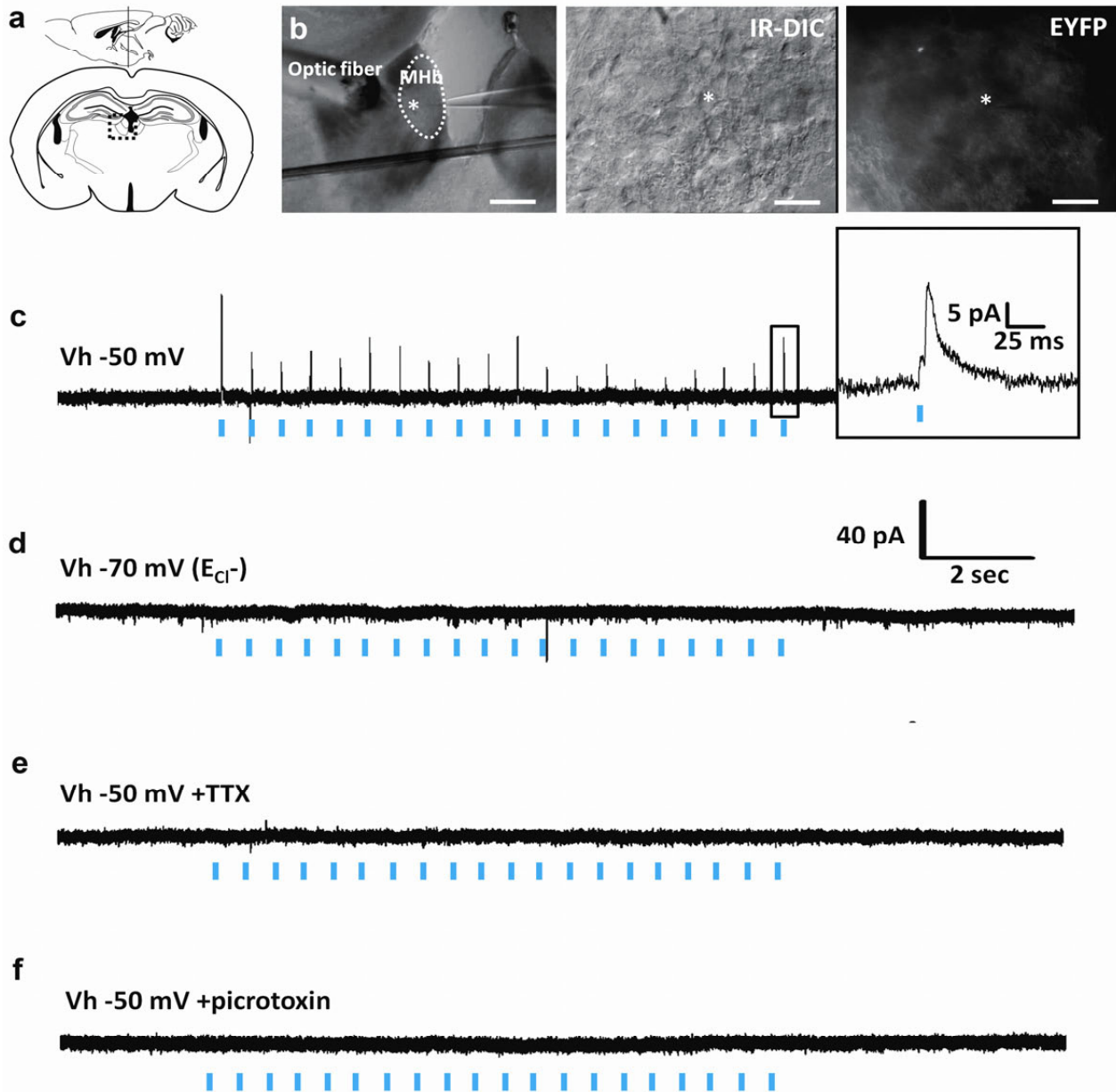


Zhao et al., Supplementary Figure 3



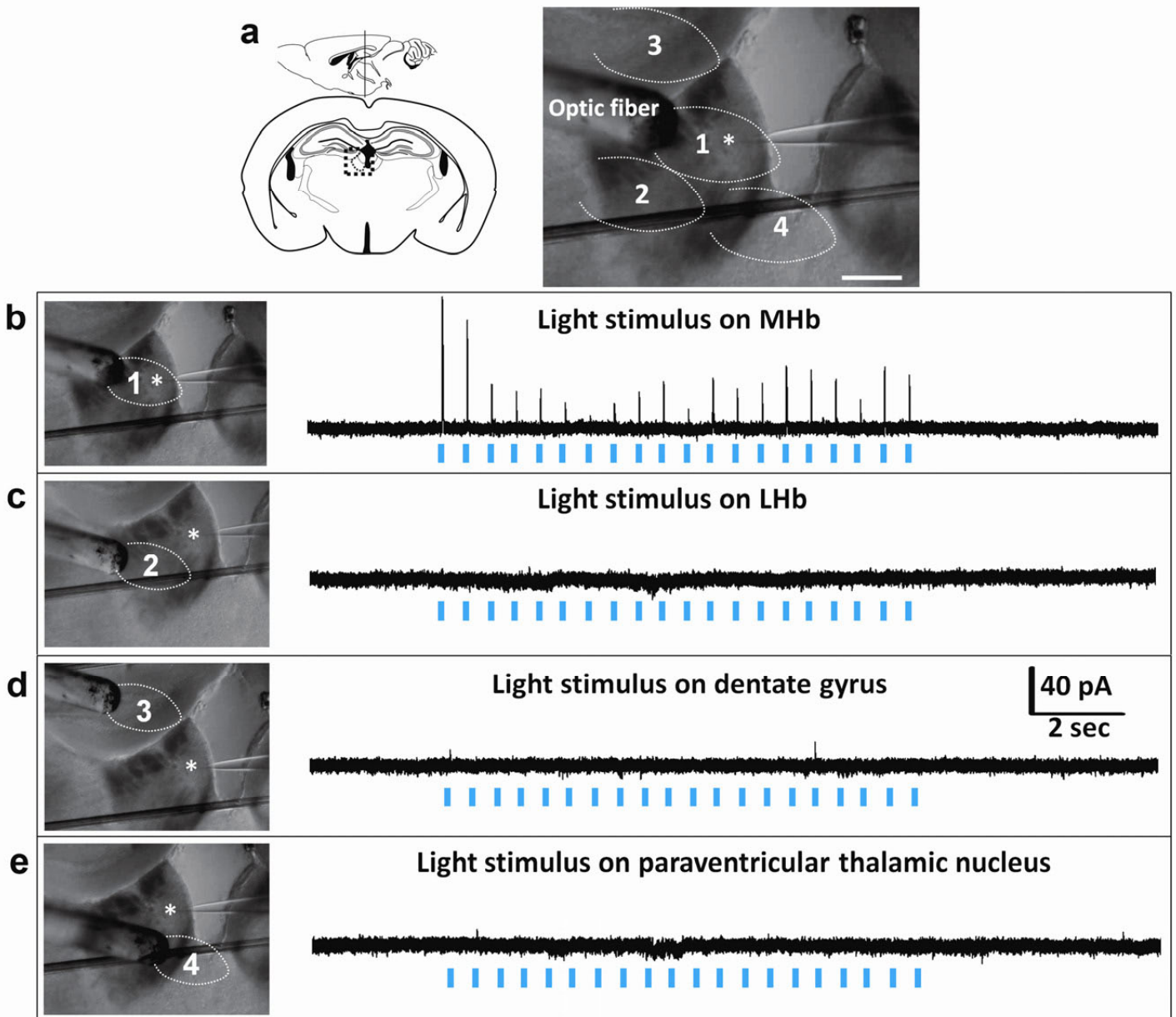
**Supplementary Figure 3.** Serial section images of fixed tissue from *VGAT-ChR2(H134R)-EYFP* line 8 BAC transgenic mouse brain. (a-k) Serial sagittal sections of native fluorescence in fixed tissue (no antibody enhancement).

## Zhao et al., Supplementary Figure 4



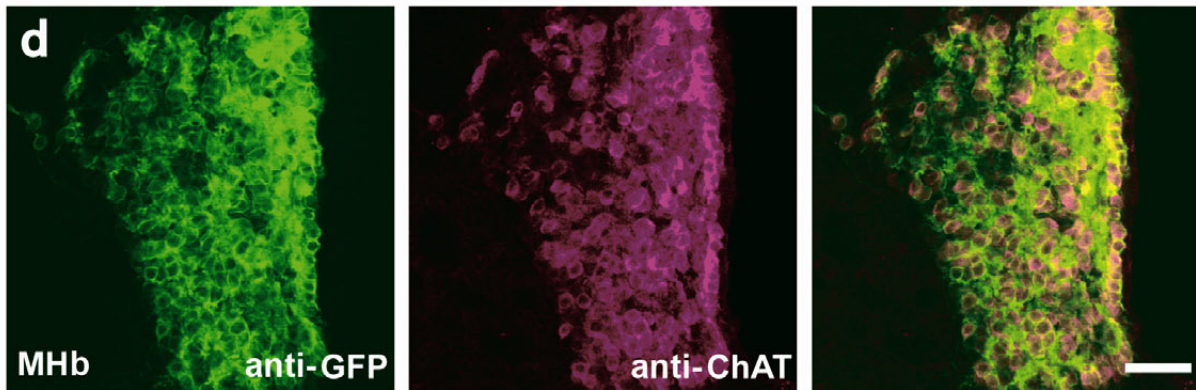
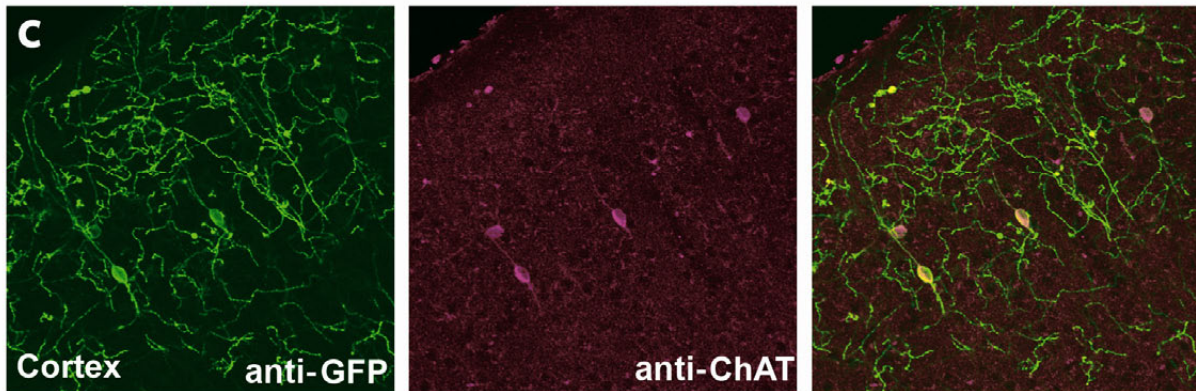
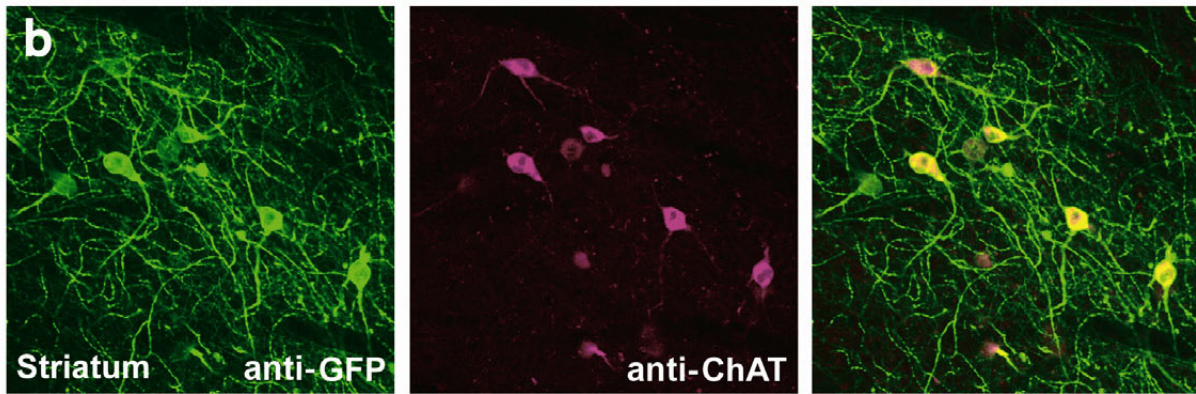
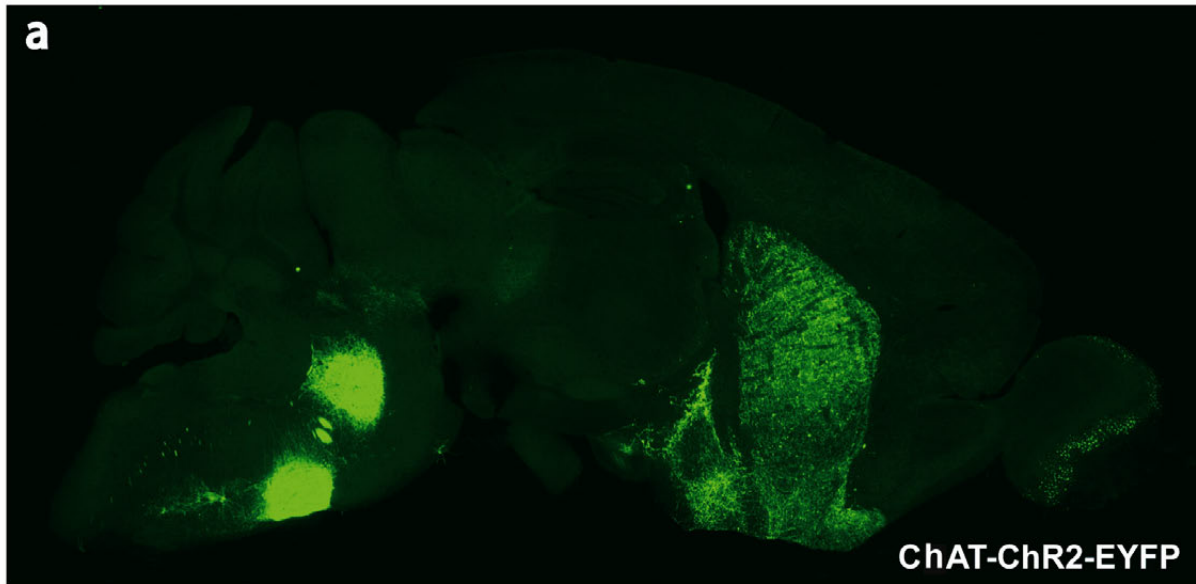
**Supplementary Figure 4.** Fast GABA-A receptor mediated synaptic currents evoked by axon terminal stimulation in acute brain slices from *VGAT-ChR2-EYFP* line 8 transgenic mice. (a) Diagram of a coronal acute brain slice containing the medial habenula (MHb, boxed region). (b) Low power image demonstrating the positioning of the optic fiber above a recorded MHb neuron (asterisk) (left). The boundary of the MHb is indicated by the dotted white line. Scale bar: 200  $\mu$ m. IR-DIC image of a recorded MHb neuron (asterisk) (middle), and corresponding EYFP image showing lack of signal from MHb somata but diffuse signal from putative ChR2-EYFP positive GABAergic axon terminal fields (right). Scale bar: 20  $\mu$ m. (c) Whole-cell voltage clamp recording (Vh -50 mV) from an MHb neuron during blue laser light stimulation applied to the MHb region (1 Hz, 2 ms pulse width, 1 mW mm<sup>-2</sup>). Blue light evokes outward currents. Inset, expanded view of an evoked outward current. (d) Repeated trial as in panel c but at Vh -70 mV (the empirically determined reversal potential for chloride ions). (e) Repeated trial as in panel c (Vh -50 mV) but with tetrodotoxin (TTX) application. TTX abolished light evoked outward currents indicating a synaptic origin of the photocurrents. (f) Repeated trial as in panel c (Vh -50 mV) but with the GABA-A receptor antagonist picrotoxin. Blue light stimulation evoked GABA release onto MHb neurons. This response was recorded from a different MHb neuron in a slice that was not exposed to TTX. The responses in panels c,d,e are recorded from a single MHb neuron.

## Zhao et al., Supplementary Figure 5



**Supplementary Figure 5.** High regional specificity of evoked GABA release by axon stimulation in the MHb in acute brain slices from *VGAT-ChR2-EYFP* line 8 transgenic mice. (a) Diagram of a coronal acute brain slice containing the medial habenula (MHb, boxed region) (Left). Low power image demonstrating the positioning of the optic fiber above a recorded MHb neuron (asterisk) (right). Four non-overlapping test regions of blue laser light stimulation are indicated and correspond to the positions marked in panels b-e. Scale bar: 200  $\mu$ m. (b) Whole-cell voltage clamp recording ( $V_h$  -50 mV) from a MHb neuron during blue laser stimulation applied to the MHb region #1 (1 Hz, 2 ms pulse width, 1 mW  $\text{mm}^{-2}$ ). Blue light evokes outward currents. (c) Repeated trial with conditions identical to panel b except that the blue laser light was applied to the lateral habenula (LHb) region #2. Blue light failed to evoke outward currents. (d) Repeated trial with conditions identical to panel b except that the blue laser light was applied to the dentate gyrus region #3. Blue light failed to evoke outward currents. (e) Repeated trial with conditions identical to panel b except that the blue laser light was applied to the paraventricular thalamic nucleus region #4. Blue light failed to evoke outward currents. Note: The responses in panels b-e were all recorded from a single MHb neuron in series.

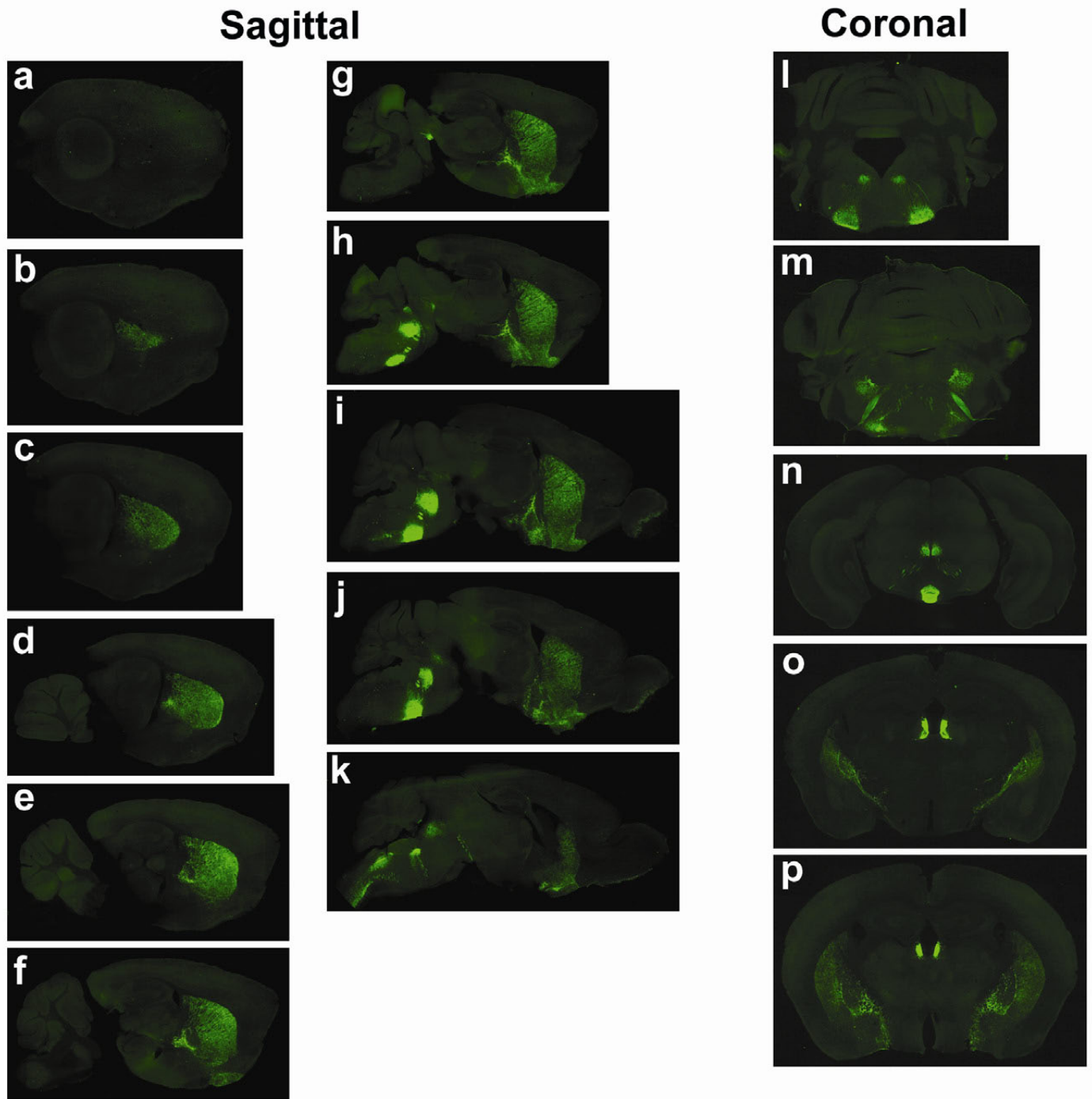
Zhao et al., Supplementary Figure 6



**Supplementary Figure 6.** Characterization of ChR2-EYFP expression in *ChAT-ChR2(H134R)-EYFP* line 6 BAC transgenic mice. **(a)** Mouse brain sagittal image showing strong ChR2-EYFP expression in the dorsal and ventral striatum, basal forebrain, facial nucleus, trochlear nucleus, various other brainstem motor neuron nuclei, and low level expression in the cortex, hippocampus, thalamus and the olfactory bulb. **(b-d)** Confocal images showing the precise colocalization of ChR2-EYFP and ChAT immunoreactivity in the striatum **(b)**, cortex **(c)** and medial habenula (MHb) **(d)**. Left panel: anti-GFP staining; middle panel: anti-ChAT staining; right panel: merged image of anti-GFP and anti-CHAT staining. Scale bar: 100  $\mu$ m.

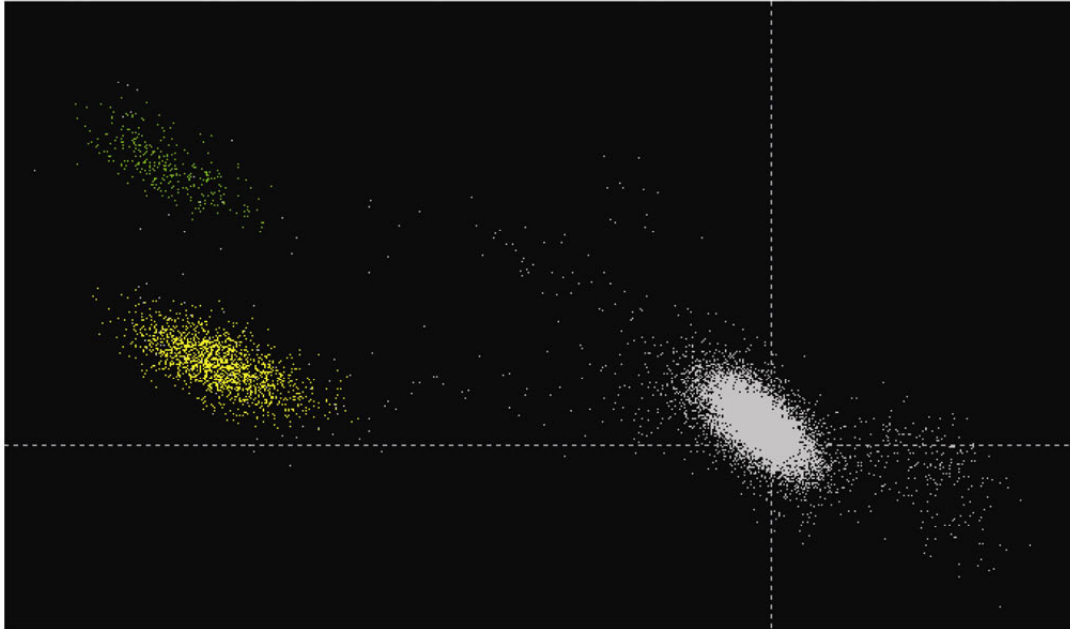


## Zhao et al., Supplementary Figure 7

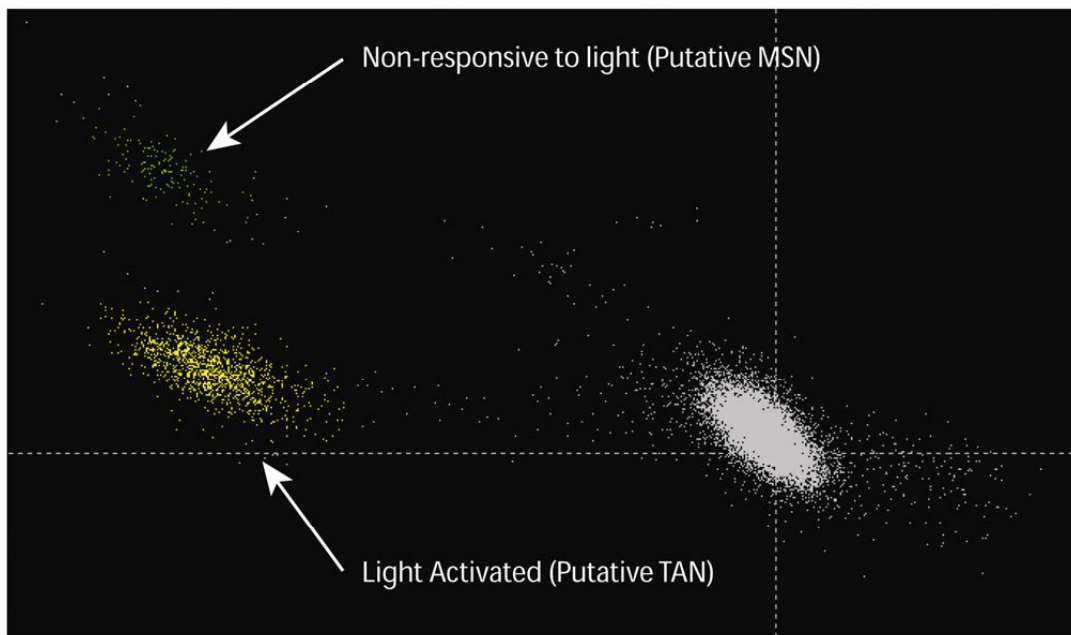


**Supplementary Figure 7.** Serial section images of fixed tissue from *ChAT-ChR2(H134R)-EYFP* line 6 BAC transgenic mouse brain. **(a-k)** Serial sagittal sections. **(l-p)** Serial coronal sections. Images represent native fluorescence in fixed tissue (no antibody enhancement).

## Laser OFF

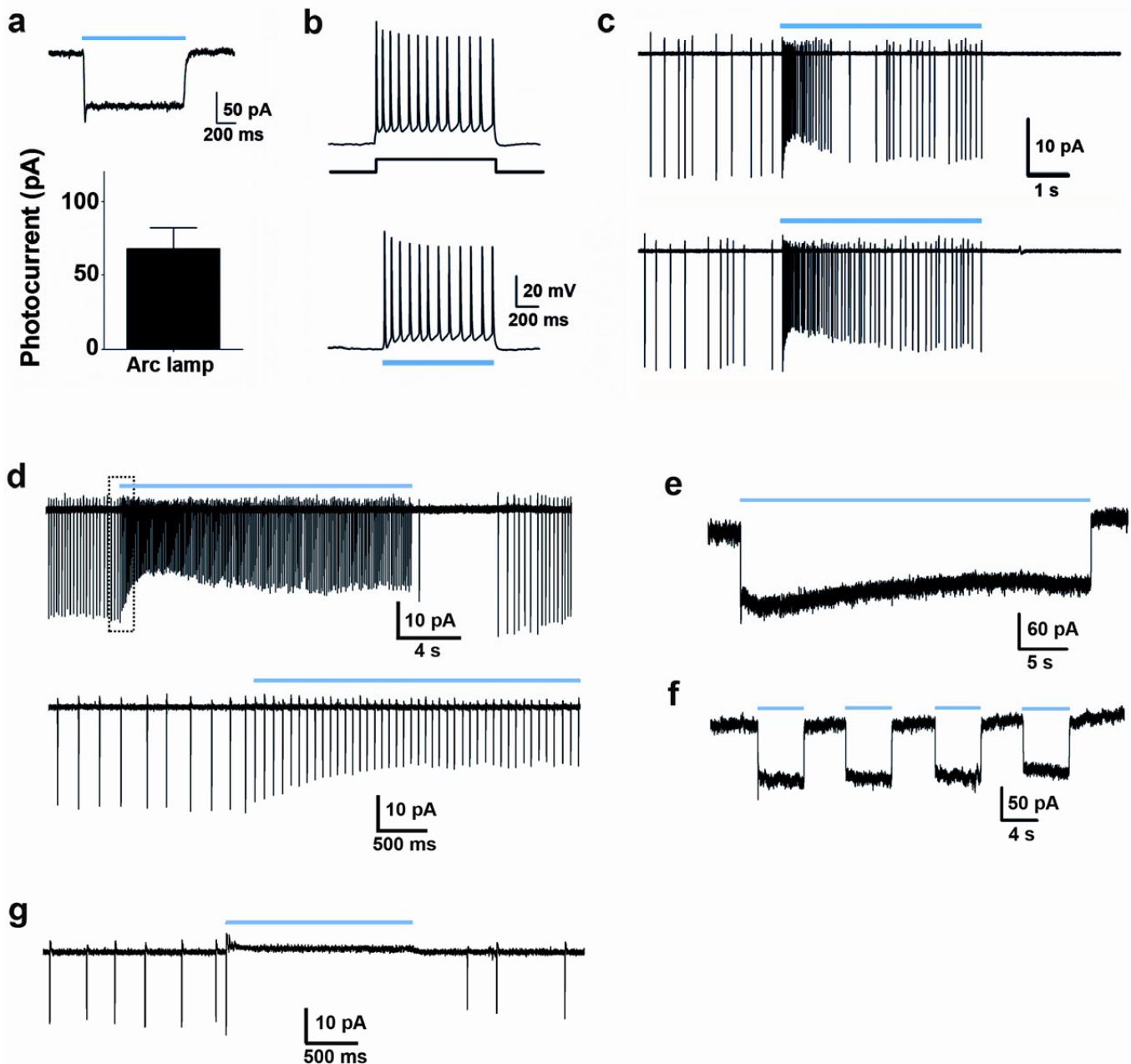


## Laser ON



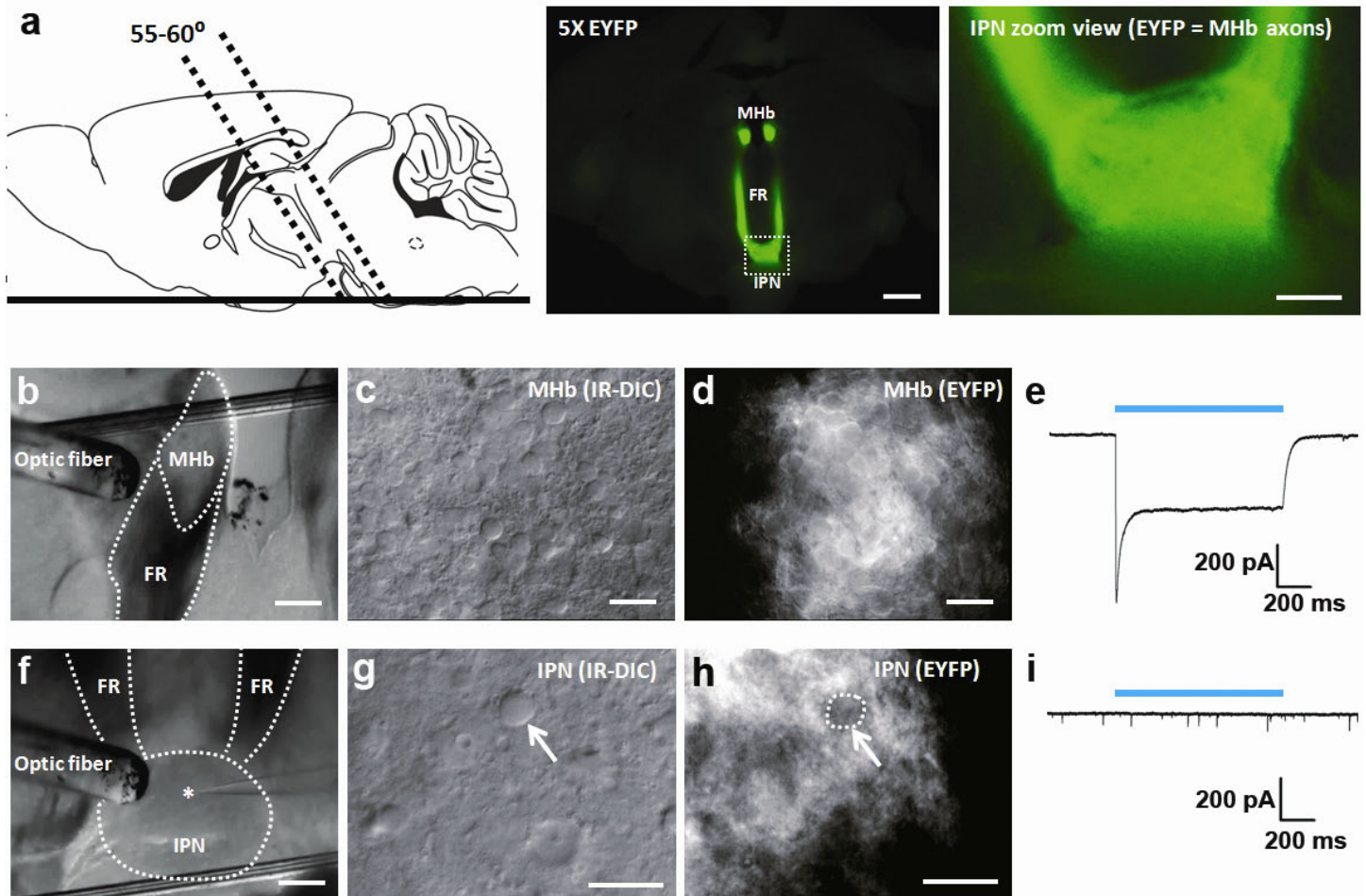
**Supplementary Figure 8.** Unaltered cluster quality during blue laser stimulation *in vivo* for *ChAT-ChR2-EYFP* line 6 transgenic mice. Two single unit clusters recorded from the dorsal striatum showing the waveform projected on the first principle component of two channels without laser stimulation (top) and with laser stimulation (bottom) during the same session. The yellow cluster on the right contained 313 waveforms occurring in a 2 ms window following the 391 pulses of blue light (18 ms pulse width at 1 Hz and 10 mW). The green cluster on the right contained one waveform occurring in the same window. Total number of waveforms for “laser off” and ‘laser on’ respectively: yellow cluster (1,577; 1,228), green cluster (308; 142), grey ‘noise’ cluster (13,595; 13,605).

## Zhao et al., Supplementary Figure 9



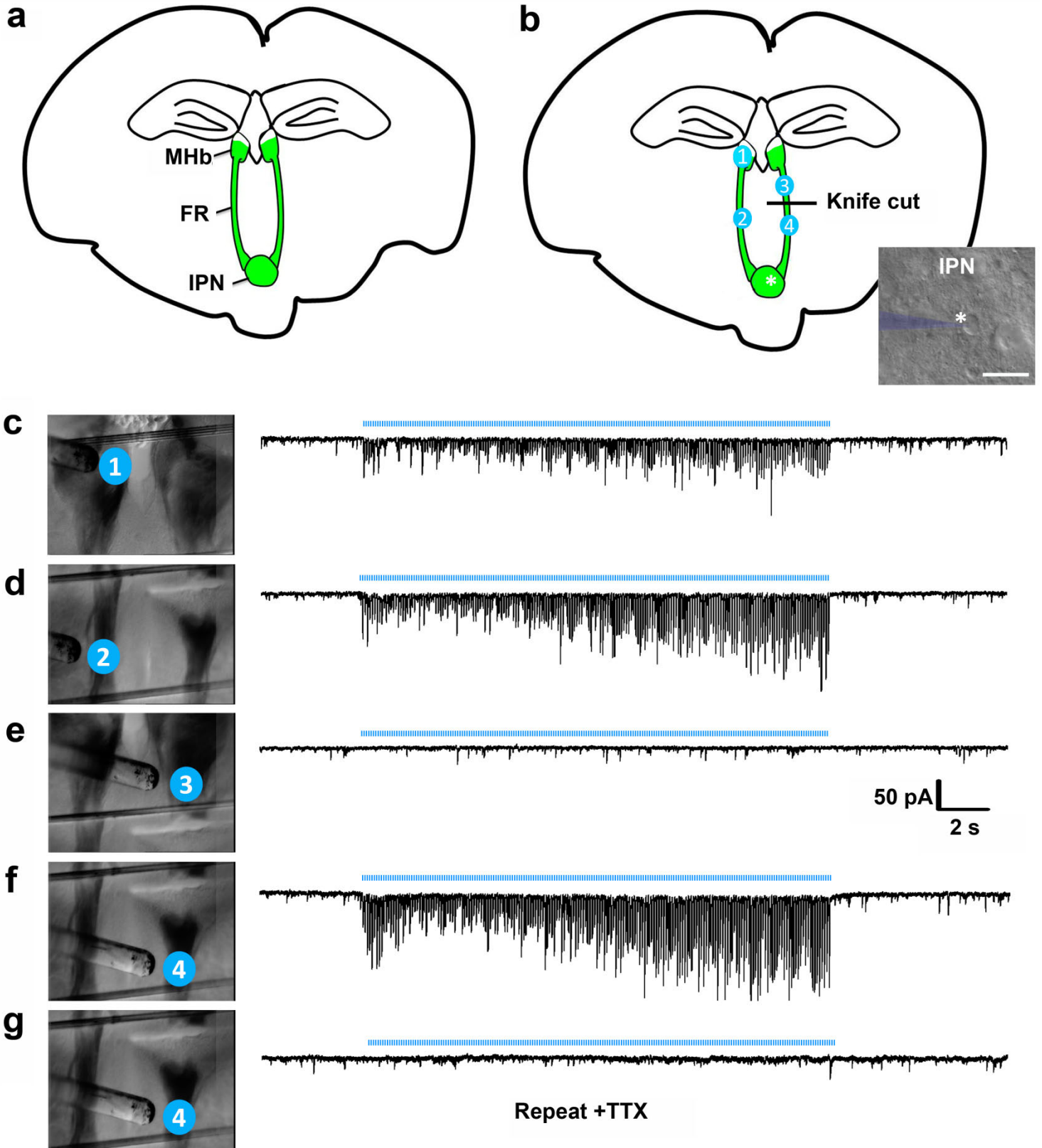
**Supplementary Figure 9.** Additional characterization of ChAT-ChR2(H134R)-EYFP BAC transgenic mouse lines. (a-f) Striatal cholinergic neuron recordings from the lower expressing *ChAT-ChR2-EYFP* line 5. (a) Example recording demonstrating photocurrent evoked by blue light (26.3 mW mm<sup>-2</sup>) (top). Summary plot of peak steady-state photocurrent in response to blue light delivered from a mercury arc lamp (bottom). (b) Current clamp mode recording showing firing in response to +80 pA current injection (top), or in response to blue laser light (26.3 mW mm<sup>-2</sup>) (bottom). (c) Example cell-attached recording demonstrating sustained facilitation of basal firing rate in response to prolonged constant blue light at 2.1 mW mm<sup>-2</sup> (top) and 10.5 mW mm<sup>-2</sup> (bottom). (d) Cell-attached recording demonstrating sustained potentiation of firing in response to 20 s of constant blue laser light (473 nm) at 26.3 mW mm<sup>-2</sup> (top). Note post-excitation pause in tonic firing. Expanded view of the response at light onset (bottom). (e) Whole cell voltage clamp recording demonstrating sustained photocurrent in response to 40 s of constant maximal blue light. (f) The response of the same neuron to repeated 5 s bouts of maximal blue light. (g) Cell-attached recording of a striatal cholinergic neuron from *ChAT-ChR2-EYFP* line 6. In contrast to panel d above, short bout of constant blue laser light at low power (2.1 mW mm<sup>-2</sup>) results in only a single action potential followed by immediate “depolarization block” of firing.

## Zhao et al., Supplementary Figure 10



**Supplementary Figure 10.** Functional ChR2-EYFP expression in MHb neurons but not IPN neurons in habenulo-peduncular acute brain slices from *ChAT-ChR2-EYFP* line 6 transgenic mice. **(a)** Diagram of the slicing angle for the habenulo-peduncular acute brain slice preparation (left). Montage image from a live brain slice showing robust EYFP fluorescence in the habenulo-peduncular pathway (middle). MHb, medial habenula; FR, fasciculus retroflexus; IPN, interpeduncular nucleus. Scale bar: 1 mm. Bright EYFP fluorescence from MHb axon terminal fields within the IPN (right). Scale bar: 200  $\mu$ m. **(b)** Low magnification image showing optic fiber placement above the MHb region. **(c)** IR-DIC image of MHb neurons. **(d)** Corresponding EYFP fluorescence from the field of view in panel c. Note the strong EYFP fluorescence around the neuronal membrane edges, indicating efficient membrane targeting of the ChR2-EYFP. **(e)** Whole-cell voltage clamp recording from a MHb neuron showing robust photocurrent in response to blue laser light (1  $\text{mW mm}^{-2}$ ). **(f)** Optic fiber placement above a recorded neuron in the IPN (asterisk). **(g)** IR-DIC image of an IPN neuron (arrow). **(h)** Corresponding EYFP fluorescence from the field of view shown in panel g. Note the strong EYFP fluorescence throughout the IPN region, but lack of discrete signal from IPN neurons (arrow). **(i)** Whole-cell recording from an IPN neuron showing no detectable photocurrent in response to blue laser light (2  $\text{mW mm}^{-2}$ ). This recording was measured in the presence of tetrodotoxin (TTX) to block synaptic activation of MHb axons. Scale bars in panels b,f: 200  $\mu$ m. Scale bars in panels c,d,g,h: 20  $\mu$ m.

Zhao et al., Supplementary Figure 11

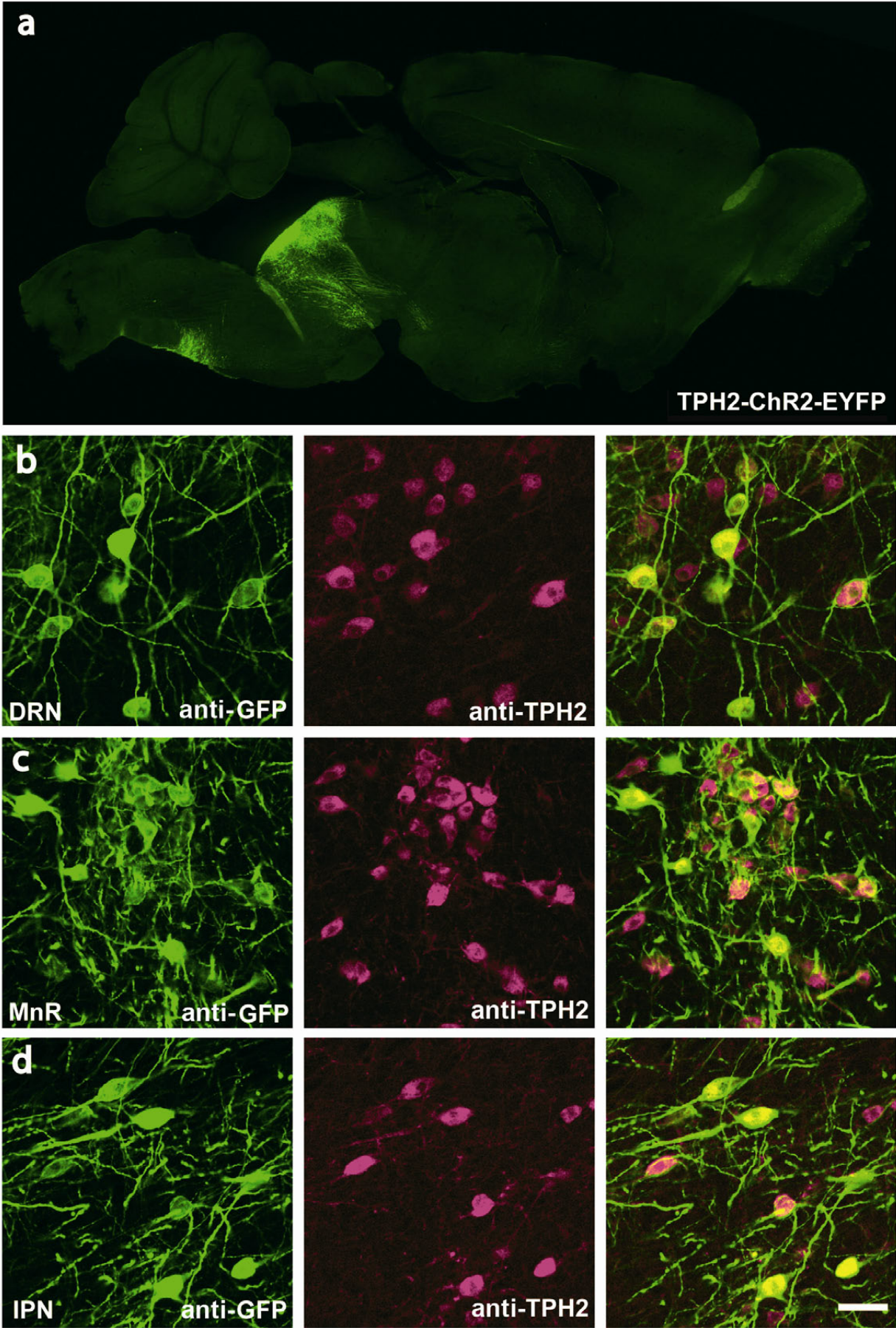


**Supplementary Figure 11.** Evidence for evoked synaptic transmission in response to blue laser stimulation of axons in *ChAT-ChR2-EYFP* line 6 transgenic mice. **(a)** Schematic of the habenulo-peduncular pathway in an acute brain slice preparation. Cholinergic neurons of the ventral 2/3 of the medial habenula (MHb) send a dense axon projection via the fasciculus retroflexus (FR) to the IPN. **(b)** A single 200  $\mu\text{m}$  brain slice containing the intact MHb-IPN projection was selected for experimentation. The brain slice contained one intact MHb-IPN pathway on each side of the brain. This feature enabled selective lesioning of the projection on one side (unilateral knife cut across the FR) while sparing the other side, thus providing a rigorous within slice control. A single IPN neuron was recorded in whole-cell voltage clamp mode ( $V_h$  -70 mV) for the entire duration of repeated probe trials consisting of patterned blue laser light stimulation (10 Hz, 2 ms pulse width, 1 mW  $\text{mm}^{-2}$ ) through a blue laser-coupled optic fiber positioned at one of four different locations as indicated (positions 1, 2, 3, or 4). The low laser power was important to restrict the spread of the laser light, thus conferring a high level of regional specificity to the light stimulus locations. (inset) Image of the recorded IPN neuron (asterisk). Scale bar: 20  $\mu\text{m}$ . **(c)** IR-DIC image of laser stimulation on the left (intact) MHb region #1 (left). Corresponding whole-cell voltage clamp recording demonstrating robust synaptic transmission evoked onto the recorded IPN neuron by sustained 10 Hz blue laser stimulation (right). **(d)** IR-DIC image of laser stimulation on the left (intact) FR axon bundle region #2 (left). Corresponding whole-cell voltage clamp recording demonstrating robust synaptic transmission evoked onto the recorded IPN neuron by sustained 10 Hz blue laser stimulation (right). NOTE: FR axon bundle stimulation consistently elicits more robust currents than direct stimulation of the MHb somata (likely due to the high convergence of axons, i.e. some axons within this slice may originate from MHb somata that were excluded from this brain slice). **(e)** IR-DIC image of laser stimulation on the right FR axon bundle region #3 above the knife cut site (left). Corresponding whole-cell voltage clamp recording demonstrating a complete loss of evoked synaptic transmission onto the recorded IPN neuron by sustained 10 Hz blue laser stimulation (right). ChR2-evoked action potentials could not propagate across the severed axon bundle. **(f)** IR-DIC image of laser stimulation on the right FR axon bundle region #4 below the knife cut site (left). Corresponding whole-cell voltage clamp recording demonstrating robust synaptic transmission evoked onto the recorded IPN neuron by sustained 10 Hz blue laser stimulation (right). With this configuration, evoked synaptic responses recorded in the IPN neuron can only arise from direct FR axon bundle stimulation with no possible contribution arising from direct blue laser stimulation of the right MHb neuron somatas. **(g)** Repeated trial as in panel f, this time in the presence of 0.5  $\mu\text{M}$  tetrodotoxin (TTX) to block sodium-dependent action potentials. TTX abolished all evoked synaptic transmission onto the recorded IPN neuron.

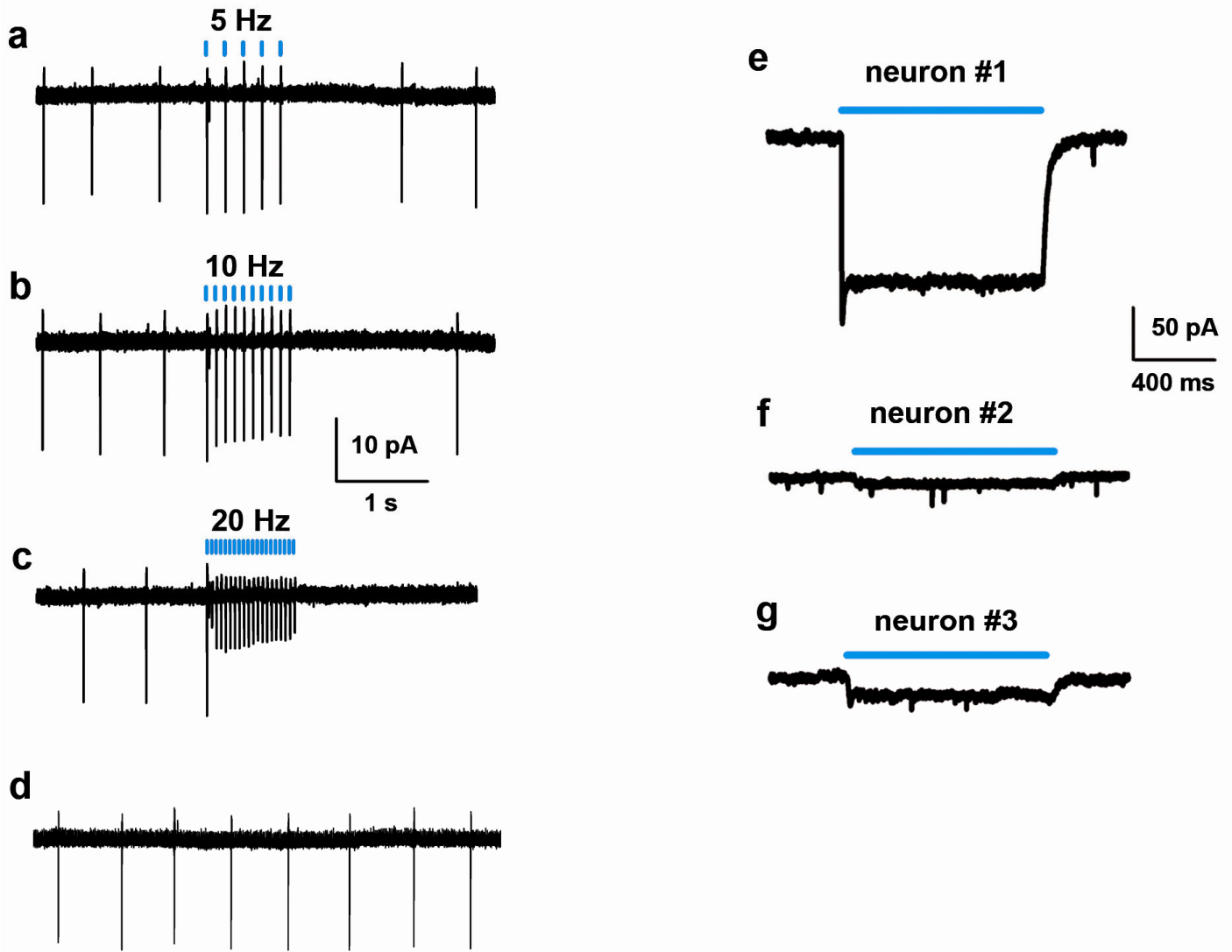
**Supplementary Figure 12.** Characterization of ChR2-EYFP expression in *TPH2-ChR2(H134R)-EYFP* BAC transgenic mice. **(a)** Mouse brain sagittal image to show the ChR2-EYFP expression in dorsal raphe nucleus, interpeduncular nucleus and gigantocellular reticular nucleus (image was enhanced with anti-GFP antibody). **(b-d)** Confocal images showing the strong colocalization of ChR2-EYFP and TPH2 in dorsal raphe nucleus (DRN) **(b)**, median raphe nucleus (MnR) **(c)** and interpeduncular nucleus (IPN) **(d)**. Left panel: anti-GFP staining; middle panel: anti-TPH2 staining; right panel: merged image of anti-GFP and anti-TPH2 staining. Scale bar: 100  $\mu\text{m}$ .

**(See next page →)**

Zhao et al., Supplementary Figure 12



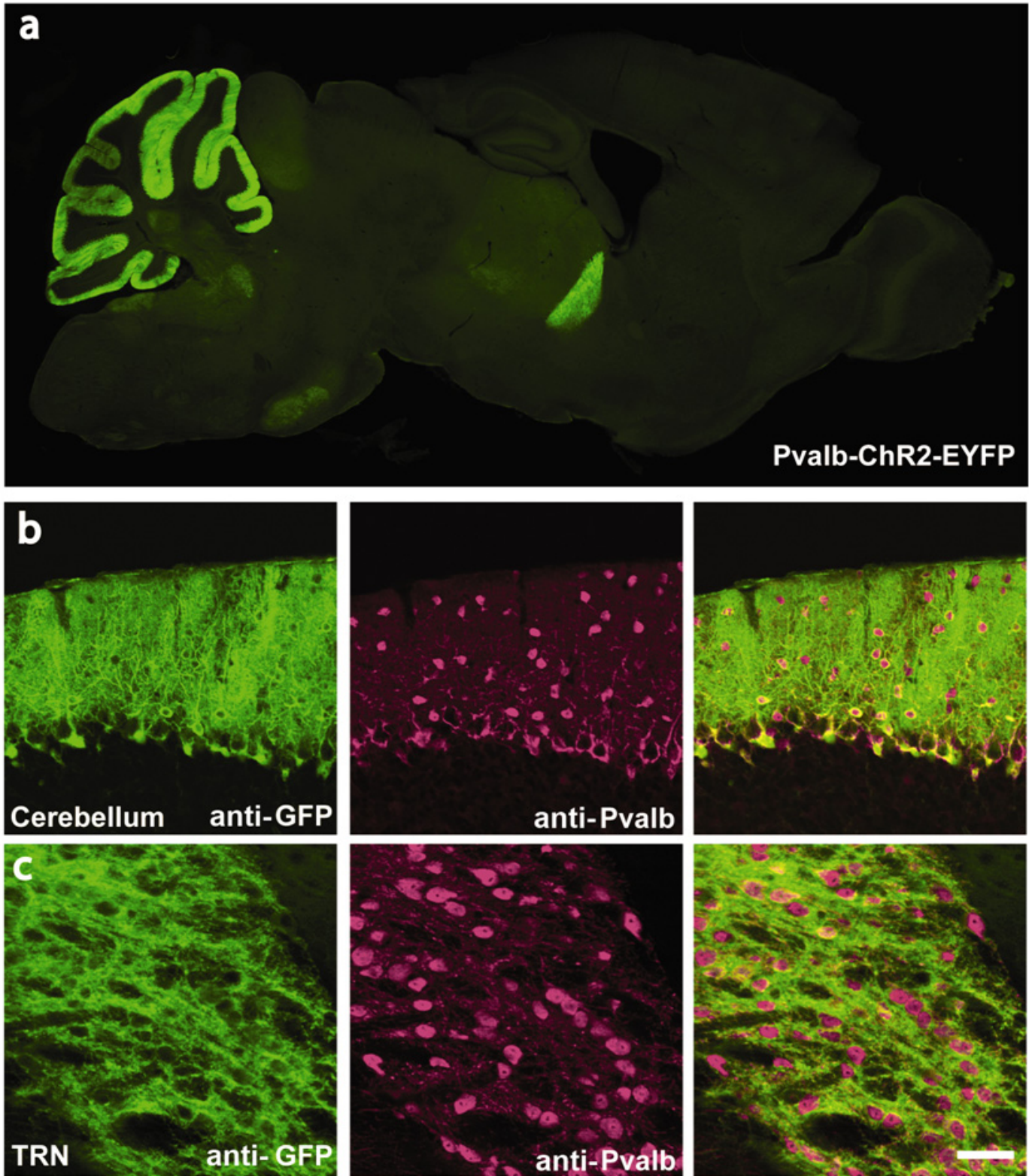
## Zhao et al., Supplementary Figure 13



**Supplementary Figure 13.** Additional characterization of TPH2-ChR2(H134R)-EYFP BAC transgenic mice. (a-d) Cell-attached recordings from a spontaneously active DRN 5-HT neuron demonstrating that patterned blue laser light stimulation can override tonic action potential firing. (a) Action potential firing in response to blue laser light (473 nm,  $2.63 \text{ mW mm}^{-2}$ ) at 5 Hz. (b) 10 Hz. (c) 20 Hz. (d) No light. (e-g) Whole cell voltage clamp recordings (-60 mV holding potential) from putative DRN 5-HT neurons. (e) Neuron #1, typical inward current in response to 1 s of blue light at maximal power for a neuron with bright EYFP fluorescence. (f,g) Neuron #2 and Neuron #3, representative traces of responses to 1 s of blue light at maximal power for neurons with no detectable EYFP fluorescence. These neurons have very low level ChR2 expression that is insufficient to significantly modulate action potential firing rate, thus demonstrating that only a subset of DRN 5-HT neurons can be robustly modulated by blue light.

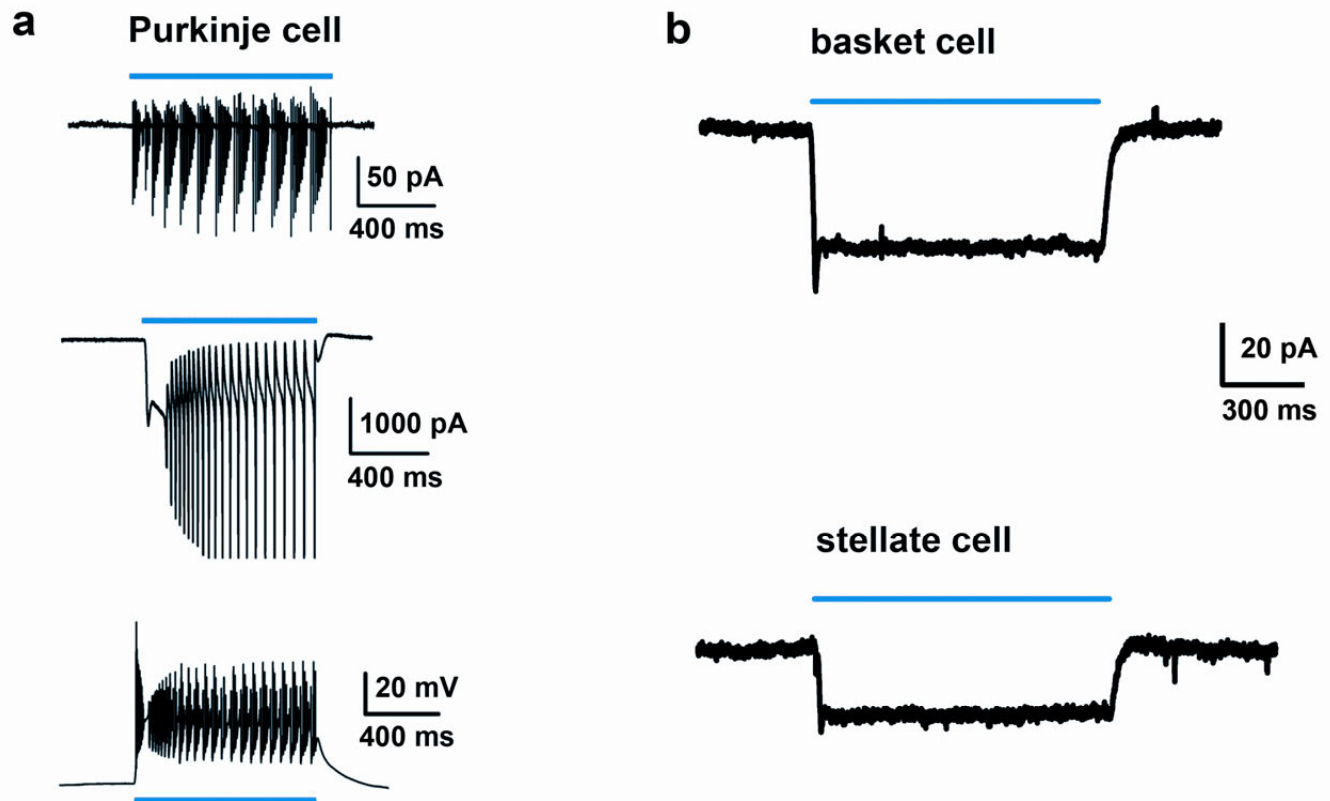


Zhao et al., Supplementary Figure 14



**Supplementary Figure 14.** Characterization of ChR2-EYFP expression in *Pvalb-ChR2(H134R)-EYFP* BAC transgenic mice. **(a)** Mouse brain sagittal image showing strong ChR2-EYFP expression in the molecular layer of the cerebellum, thalamic reticular nucleus (TRN), brainstem, and low level expression in the thalamus and the inferior colliculus. **(b-,c)** Confocal images showing colocalization of ChR2-EYFP and Parvalbumin in the molecular layer of the cerebellum **(b)** and the TRN **(c)**. Left panel: anti-GFP staining; middle panel: anti-Parvalbumin staining; right panel: merged image of anti-GFP and anti-Pvalb staining. Scale bar: 100  $\mu$ m.

## Zhao et al., Supplementary Figure 15



**Supplementary Figure 15.** Additional functional characterization of *Pvalb-ChR2(H134)-EYFP* BAC transgenic mice. (a) Strong ChR2-EYFP expression combined with high power light stimulation in some Purkinje cells led to observations of complex spikes in cell-attached (top), whole cell voltage clamp (middle), and whole cell current clamp (bottom) modes. Complex spikes consisted of initial simple spikes with superimposed TTX-insensitive putative dendritic  $\text{Ca}^{2+}$  spikes. (b) Voltage-clamp recording of a basket cell in the inner molecular layer of the cerebellum demonstrating photocurrent in response to 1 s of blue light from a mercury arc lamp (top). Voltage-clamp recording of a stellate cell in the outer molecular layer of the cerebellum demonstrating photocurrent in response to 1 s of blue light (bottom). Note: the level of ChR2-EYFP expression is more than an order of magnitude lower than that of Purkinje cells in this line, as determined by comparing maximal photocurrent amplitude.

## Zhao et al., Supplementary Table 1

**Supplementary Table 1.** Generation and initial characterization of cell-type specific Chr2 BAC transgenic mouse lines

Lines	BAC clone ID	Targeted Exon	Transgenic founders	Lines w/Tg expression	Strongest Expression
VGAT-ChR2(H134R)-EYFP	RP23-392P11	exon I	10	4 (#8, 6, 9, 3)	Line 8
ChAT-ChR2(H134R)-EYFP	RP23-246B12	exon III	18	3 (#6, 5, 9)	Line 6
TPH2-ChR2(H134R)-EYFP	RP23-112F24	exon I	7	1 (#5)	Line 5
Pvalb-ChR2(H134R)-EYFP	RP23-305H12	exon II	10	6 (#1, 5, 9, 10, 12, 15)	Line 15

## Zhao et al., Supplementary Table 2

**Supplementary Table 2.** Genotyping of cell-type specific Chr2 BAC transgenic mouse lines.

Lines	Primers	Primer sequences	PCR product
VGAT-Chr2(H134R)-EYFP	VGAT8 hChr2R1	5' ACCCTTCTGTCCTTTCTCC 3' 5' GCAAGGTAGAGCATAGAGGG 3'	500 bp
ChAT-Chr2(H134R)-EYFP	ChAT5 hChr2R1	5' TCTGTTCCCGGTCGGCAGC 3' 5' GCAAGGTAGAGCATAGAGGG 3'	500 bp
TPH2-Chr2(H134R)-EYFP	TPH5 hChr2R1	5' GCTGAGAAAGAAAATTACATCG 3' 5' GCAAGGTAGAGCATAGAGGG 3'	500 bp
Pvalb-Chr2(H134R)-EYFP	Prv5 hChr2R1	5' CTTTTCGCACTTGCTCTGC 3' 5' GCAAGGTAGAGCATAGAGGG 3'	550 bp

## Zhao et al., Supplementary Table 3

Supplementary Table 3. Co-localization of ChR2-EYFP and cell-type specific markers in ChR2-EYFP BAC transgenic lines

	VGAT-ChR2-EYFP		ChAT-ChR2-EYFP		TPH2-ChR2-EYFP		Pvalb-ChR2-EYFP	
	GAD67/YFP <sup>a</sup>	YFP/GAD67 <sup>a</sup>	ChAT/YFP	YFP/ChAT	TPH2/YFP	YFP/TPH2	Pvalb/YFP	YFP/Pvalb
<i>Cortex</i>	279/301 (92.7%)	311/324 (96%)	93/121 (76.9%) <sup>b</sup>	72/72 (100%) <sup>b</sup>				
<i>Hippocampus</i>	119/128 (93%)	151/179 (84.4%)						
<i>Striatum</i>			261/261 (100%)	261/261 (100%)				
<i>Inferior Colliculus</i>	105/113 (92.9%)	117/132 (88.6%)						
<i>Purkinje Cells</i>	120/120 (100%)	120/120 (100%)					150/150 (100%)	150/150 (100%)
<i>MHb</i>			393/403 (97.5%)	391/398 (98.2%)				
<i>DRN</i>					151/151 (100%)	209/258 (81.0%)		
<i>MnR</i>					145/145 (100%)	210/241 (87.1%)		
<i>IPN</i>					130/132 (98.5%)	198/233 (85.0%)		

**Note a:** GAD67/YFP = number (%) of ChR2-EYFP positive cells that are also GAD67 staining positive; YFP/GAD67 = number (%) of GAD67 staining positive cells that are also ChR2-EYFP positive. The same definition is used for all other transgenic lines and columns.

**Note b:** Anti-ChAT immunofluorescence signal in cortical neurons is very weak. Some of the neurons have bright enough ChAT signal for quantification, but some of them are close to background. So for the neurons clearly ChAT positive, they are all ChR2-EYFP positive (100%); but some of the ChR2-EYFP positive neurons did not show clear anti-ChAT immunofluorescence signal.

**Abbreviation:** MHb, medial habenula; DRN, dorsal raphe nucleus; MnR, median raphe nucleus; IPN, interpeduncular nucleus.